

## Original Article

# miR-132/212 cluster inhibits the growth of lung cancer xenografts in nude mice

Judong Luo<sup>1\*</sup>, Cuicui Meng<sup>1\*</sup>, Yiting Tang<sup>1</sup>, Shuyu Zhang<sup>2</sup>, Meizhen Wan<sup>3</sup>, Yanzhi Bi<sup>4</sup>, Xifa Zhou<sup>1</sup>

<sup>1</sup>Department of Radiotherapy, Changzhou Tumor Hospital, Soochow University, Changzhou 213001, China; <sup>2</sup>School of Radiation Medicine and Protection and Jiangsu Provincial Key Laboratory of Radiation Medicine and Protection, Soochow University, Suzhou 215123, China; <sup>3</sup>Department of Pathology, Changzhou Tumor Hospital, Soochow University, Changzhou 213001, China; <sup>4</sup>Department of Oncology, Changzhou Tumor Hospital, Soochow University, Changzhou 213001, China. \*Equal contributors.

Received September 2, 2014; Accepted October 23, 2014; Epub November 15, 2014; Published November 30, 2014

**Abstract:** Objective: Lung cancer remains the leading cause of cancer-related death worldwide and microRNAs (miRNAs) play important roles in lung cancer progression. In this study, we investigate the effects of miR-132/212 cluster on the growth of subcutaneous xenografts of human lung cancer H1299 cells in nude mice, and further explore the underlying mechanisms. Methods: Nude mice with subcutaneous transplantation tumor of human lung cancer H1299 cells were randomly divided into three groups: the sham group, the control vector group, and the microRNA-132/212 group. The control vector and microRNA-132/212 cluster plasmid was intratumoral injected respectively. Tumor volume was measured during the intervention process, with a tumor growth curve generated. Immunohistochemistry was performed to analyze the expression level of Ki-67, P21, CyclinD1 and CD31 in each group. Results: The tumor volume of miR-132/212 group was significantly smaller than that of the control group at the terminal time point ( $P < 0.05$ ). The expression levels of Ki-67, CyclinD1 and CD31 in the miR-132/212 group was significantly lower than the control group ( $P < 0.05$ ), while the expression levels of P21 in the miR-132/212 group were significantly higher than the control group ( $P < 0.05$ ). Conclusion: miR-132/212 cluster significantly inhibited the growth of subcutaneous xenografts of human lung cancer H1299 cells in nude mice. The inhibitory effect of miR-132/212 cluster in tumor growth may be mediated by upregulating the expression of P21 and down-regulating the expression of CyclinD1, thereby inhibiting tumor tissue proliferation and angiogenesis and resulting in the inhibition of tumor growth.

**Keywords:** Lung cancer, miR-132/212 cluster, P21, CyclinD1, angiogenesis

## Introduction

microRNAs (miRNAs) are a class of endogenous non-coding RNAs of approximately 22 nt in length. After the first discovery of the small RNAs encoded by the *lin-4* gene in *C. elegans* [1], there was an explosion in the field of miRNA biology in the subsequent years across different species. miRNAs can induce the degradation or translation inhibition of a target mRNA by specifically binding to the target mRNA sequence, thereby regulating gene expression and modulating a set of biological processes [2, 3]. Certain miRNAs have additional roles as oncogenes or tumor suppressor gene [4]. The expression levels of miRNAs are closely correlated with tumor development and progression [5, 6].

miR-132 and miR-212, collectively termed the miR-132/212 cluster, are encoded in the same intron of a non-coding gene on chromosome 17 in humans. Studies have shown that the miR-132/212 cluster is involved in the vascular smooth muscle dysfunction mediated by angiotensin II (Ang-II) [7]. The overexpression of miR-132/212 cluster in pancreatic adenocarcinoma tissues suppress the expression of the retinoblastoma tumor-suppressor gene (*Rb1*) and stimulate the proliferation of pancreatic cancer Panc-1 cells [8]. However, the effect of miR-132/212 cluster on the malignant biological behavior of lung cancer remains unclear. The purpose of this study was to reveal the effect of miR-132/212 cluster on the growth of subcutaneous xenografts of human lung cancer H1299

cells in nude mice and further investigate the possible mechanisms.

## Materials and methods

### *Animals and reagents*

5-week-old BALB/c nude mice were purchased from Shanghai SLAC Laboratory Animal Co., Ltd. (Shanghai, China). The mice were housed in individually ventilated cages (IVCs) in the Animal Laboratory of the Radiation Medicine and Protection, Medical College of Soochow University, and were given *ad libitum* access to sterilized diet and water. The plasmids used in this study were synthesized by GenePharma Co. Ltd. (Shanghai, China). Cells were transfected with constructed vectors by Lipofectamine 2000 (Invitrogen, Calsbad, CA). The rabbit anti-P21 antibody, rabbit anti-CD31 antibody (Epitomics, Burlingame, CA), rabbit anti-CyclinD1 antibody (Santa Cruz Biotechnology, Santa Cruz, CA), rabbit anti-Ki-67 antibody (Guge Biotech, Wuhan, China) were incubated at a 1:50-1:800 dilution at 4°C overnight. The immunohistochemical streptavidin peroxidase-conjugated (SP) kit and DAB substrate kit were purchased from Beijing Zhongshan Golden Bridge Biotech Co., Ltd.

### *Cell culture and plasmids extraction*

Human lung cancer H1299 cells were cultured in high-glucose Dulbecco's modified Eagle media (DMEM) with 10% Fetal Bovine Serum. Cells were maintained in an incubator at 37°C with 5% CO<sub>2</sub>. Cell culture media was changed every two days. Cells were resuspended and cultured when reaching 80 to 90% confluence. Plasmids were extracted according to the protocol of the Large-scale Endotoxin-free Plasmid Extraction Kit (Kangwei, Beijing China.). The concentration of the control vector and miR-132/212 plasmid used in this study was 299.7 µg/ml and 235 µg/ml respectively.

### *Establishment of a lung cancer subcutaneous tumor xenograft model in nude mice and plasmid intervention*

Cells in the logarithmic growth phase were trypsinized using 0.25% trypsin and then centrifuged.  $4 \times 10^6$  H1299 cells were suspended in 100 µl PBS and then inoculated subcutaneously into the right posterior flank region of

BALB/c nude mice. When the tumor volume reached 100-150 mm<sup>3</sup>, the mice were randomly divided into three groups: the sham group, the control vector group and the miR132-212 group and plasmids (2 µg) were injected intratumor respectively at multiple positions. Plasmid transfection was performed every five days, for a total of four times. Mice in the control group received no intervention. From the day of intervention, the longest diameter (a) and the shortest diameter (b) of the tumor were measured with a electronic caliper every three days, and the tumor volume ( $V = 0.5 \times a \times b^2$ ) was calculated. The mental state, feeding, activity, urine and feces of those nude mice were observed during the experiment. The tumor surface for ulcers or infections was inspected. Three days after the last intervention, mice were euthanized by cervical dislocation. Tumor samples were excised, fixed in 4% paraformaldehyde, and cut into 4-µm serial sections. The animal studies were performed following the institutional guidelines approved by the Ethical Committee of Soochow University.

### *Immunohistochemistry analysis*

The SP method [9] was performed to detect the expression of Ki-67, P21, CyclinD1 and CD31 in each group. Briefly, the paraffin sections were placed in an oven at 60°C for 1 h and then rehydrated in a graded ethanol series (100%, 95%, 90%, 85%, 70%). Citrate buffer was used for heat-induced antigen retrieval. 3% H<sub>2</sub>O<sub>2</sub> was used to block the endogenous peroxidase. Then goat serum was used as a blocking solution before the primary antibody applied. The sections were refrigerated with the rabbit anti-Ki-67 (1:800 dilution) primary antibodies, rabbit anti-P21 (1:150 dilution) primary antibodies, rabbit anti-CyclinD1 (1:100 dilution) primary antibodies, and rabbit anti-CD31 (1:50 dilution) primary antibodies at 4°C overnight. The samples were re-warmed at 37°C for 1 h, washed with PBS, and incubated in a biotinylated goat anti-rabbit secondary antibody working solution. After incubated with horseradish peroxidase (HRP)-conjugated streptavidin, the sections were stained using 3, 3'-diaminobenzidine (DAB) as selenium organic reagent to reveal the antibody expression. Meanwhile, the nucleus was stained with hematoxylin. The hematoxylin staining was smoothed with hydrochloric acid alcohol, and restrained blue in 50°C warm

## miR-132/212 cluster inhibits lung cancer xenografts proliferation



**Figure 1.** Subcutaneous xenograft of human lung cancer H1299 cells in nude mice. A. Representative subcutaneous xenograft from the mice of each group at the end time-point; B. Representative tumors excised from the mice of each group.  $4 \times 10^6$  cells were suspended in 100  $\mu$ l PBS and then inoculated subcutaneously into the right posterior flank region of BALB/c nude mice. At the terminal point when the mice were sacrificed, tumors were photographed and excised in the Laminar Flow.

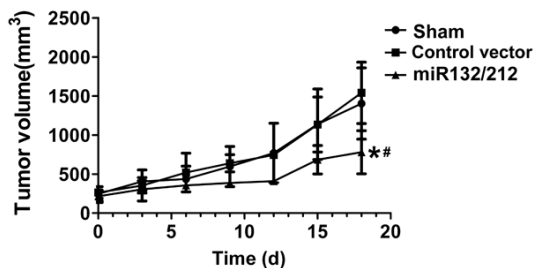


**Figure 2.** The growth curve of subcutaneous xenografts of human lung cancer H1299 cells. The tumor size was measured at a 3 day intervals. \* $P < 0.05$ , compared with the sham group; # $P < 0.05$ , compared with the control vector group. Control vector (2.0  $\mu$ g) and miR132/212 (2.0  $\mu$ g) were injected intratumor respectively together with transfection reagents once every five days with a total of four interventions.

water. Slides were hydrated with an ethanol gradient, cleared in xylene, and coverslipped using mounting solution with neutral balsam. Images were taken under an optical microscope.

### Calculation and quantification of protein expression

Evaluation and calculation of positive results: Ki-67 was localized in the nucleus of tumor cells with brown staining. Five fields from each

slice were randomly selected using an objective with 200 $\times$  magnification. Proliferation index (PI) was calculated according to the following formula:  $PI = \text{Ki-67-positive cells}/\text{total cells} \times 100\%$ . P21 and CyclinD1 were localized in the nuclei of tumor cells with brown staining. Five fields from each slice were randomly selected for imaging at 200 $\times$  magnification. Image-Pro Plus 6.0 was used to measure the average optical density of positive expression in lung cancer xenografts in nude mice of each group.

CD31, which was used to label the tumor blood vessels, was stained as a marker of tumor microvessel density (MVD) count: Positive staining was localized in the cytoplasm of endothelial cells with brown staining. Single endothelial cells, cell clusters or unconnected single vessels stained in brown were counted as vessels. The vascular intensive area, i.e., the hot zone, was identified at low magnification for each slice. The number of vessels was counted with five randomly selected fields at high magnification (200 $\times$ ). The average value was calculated.

### Statistical analysis

Statistical analysis was performed using SPSS 19.0 software. All data are presented as the mean  $\pm$  SD. Comparisons among groups were performed using one-way analysis of variance (ANOVA), and comparisons between pairs of groups were examined using the LSD-t test.  $P < 0.05$  was considered statistically significant.

## Results

### miR-132/212 cluster inhibits the lung cancer H1299 cells subcutaneous xenograft growth in nude mice

Tumor growth in the miR-132/212 group was slower than in the sham and control vector group. The tumor growth curve for the miR-132/212 group was flat. At the terminal point when the mice were sacrificed, the tumor volume of each groups were excised and calculated: the sham group:  $(1403.33 \pm 456.19)$  mm<sup>3</sup>, the control vector group:  $(1540.24 \pm 392.35)$  mm<sup>3</sup> and miR-132/212 group:  $(779.29 \pm 276.45)$  mm<sup>3</sup>. There was no significant difference in tumor volume between the sham group and control vector group ( $P > 0.05$ ). The tumor volume for the miR-132/212 group was significantly smaller than that of the sham group ( $P <$

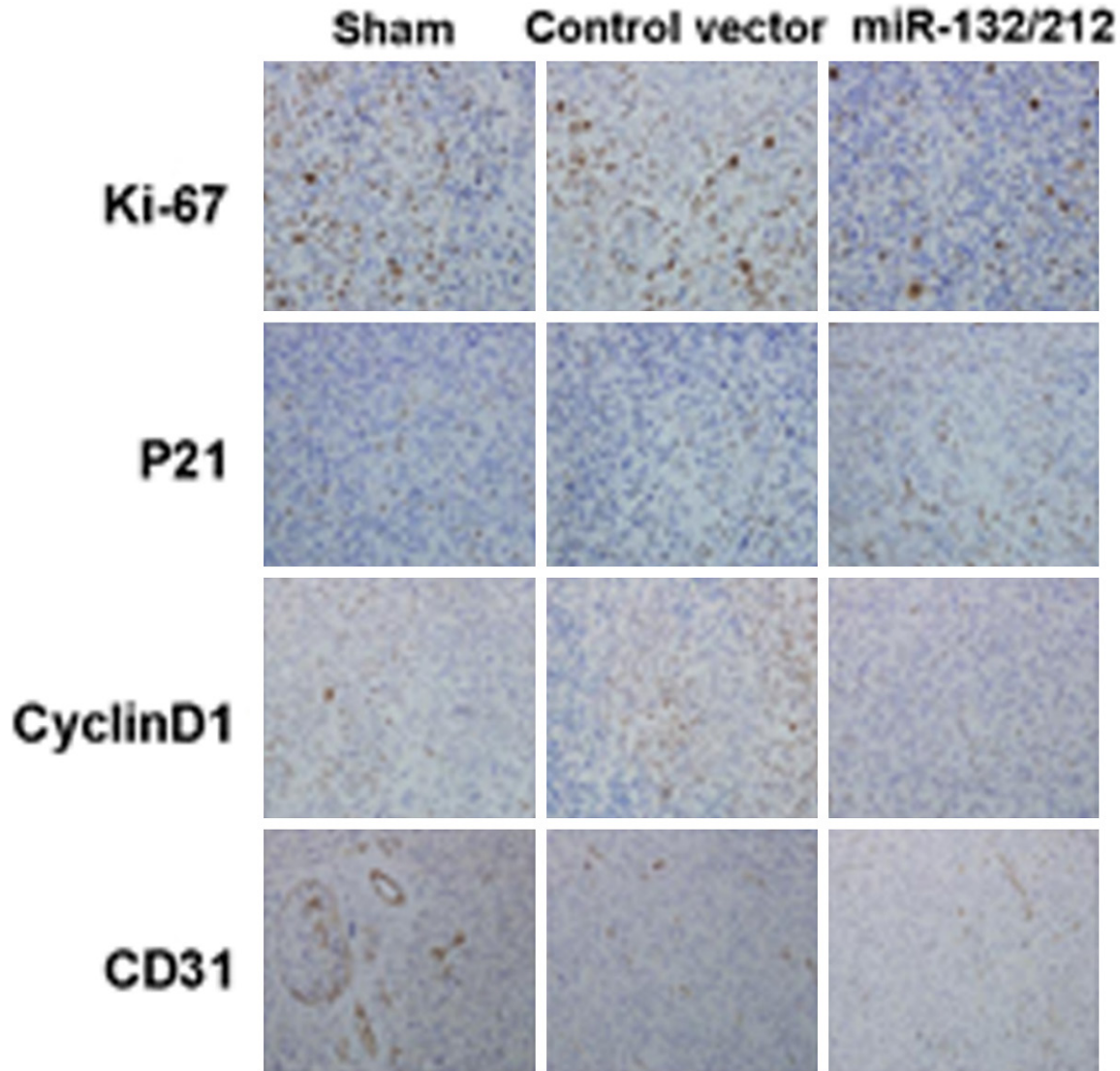


**Figure 3.** Representative immunohistochemistry staining images of Ki-67, P21, CyclinD1 and CD31 from sample tissue in each group. The primary antibody Ki-67 was diluted at 1:800, P21 diluted at 1:150, CyclinD1 diluted at 1:100, CD31 diluted at 1:50. (Figures are photographed at a 200× magnification).

**Table 1.** The average optical density of protein expression levels of P21 and CyclinD1 in each group (n=4,  $\bar{x} \pm SD$ )

Group	P21 ( $\times 10^{-3}$ )	CyclinD1 ( $\times 10^{-3}$ )
Sham	3.2 $\pm$ 0.90	4.7 $\pm$ 1.19
Control vevtor	3.1 $\pm$ 1.24	6.8 $\pm$ 1.88
miR-132/212	11.7 $\pm$ 2.05* <sup>#</sup>	2.7 $\pm$ 0.77* <sup>#</sup>

\* $P < 0.05$ , compared with the sham group; <sup>#</sup> $P < 0.05$ , compared with the control vector group.

0.05) or the control vector group ( $P < 0.05$ , **Figures 1** and **2**). The results indicated that miR-132/212 cluster inhibits the lung cancer

H1299 cells subcutaneous xenograft growth in nude mice.

*miR-132/212 cluster decreases the expression of CyclinD1 and increases the expression of P21 in tissues from subcutaneous xenografts of human lung cancer cells*

P21 and CyclinD1 were expressed in the nuclei of tumor cells, as shown with brown staining (**Figure 3**). Immunohistochemical analysis indicated that the expression of P21 in the miR-132/212 group was stronger than the control vector group, while the expression of CyclinD1

## miR-132/212 cluster inhibits lung cancer xenografts proliferation

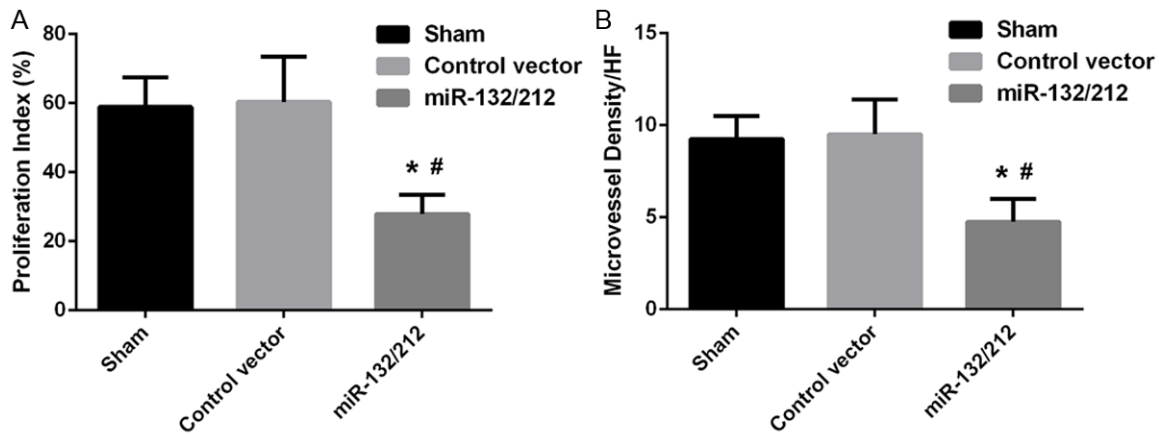


**Figure 4.** Quantification of immunohistochemistry analysis of proliferation index and microvessel density (MVD). A. Tumor proliferation index of each group; B. MVD count of each group. \* $P < 0.05$ , compared with the sham group; # $P < 0.05$ , compared with the control vector group.

in the miR-132/212 group was slighter than the control vector group (Figure 3).

We further quantification the expression level of P21 and CyclinD1. As show in Table 1, the expression of P21 in the miR-132/212 group was significantly higher than that of the sham group ( $P < 0.05$ ) or the control vector group ( $P < 0.05$ ), while the expression of CyclinD1 in the miR-132/212 group was significantly lower than the sham group ( $P < 0.05$ ) or the control vector group ( $P < 0.05$ ). All these results demonstrated that miR-132/212 cluster inhibits the H1299 subcutaneous xenograft growth via up-regulating the expression of P21 and down-regulating the expression of CyclinD1.

### *miR-132/212 cluster decreases the proliferation index and the forming of tumor angiogenesis*

Analysis of the immunohistochemical results showed that the cell proliferative index for the sham group, control vector group and miR-132/212 group were (58.89 ± 8.60%), (60.36 ± 13.09%), (27.89 ± 5.63%), respectively. The tumor cell proliferation index for the miR-132/212 group was significantly lower than the sham group ( $P < 0.05$ ) or the control vector group ( $P < 0.05$ , Figures 3 and 4).

The MVDs in the sham, control vector, and miR-132/212 groups were (9.25 ± 1.26)/HF, (9.50 ± 1.91)/HF, and (4.75 ± 1.26)/HF, respectively. The MVDs in the miR-132/212 group were significantly lower than the sham group ( $P < 0.05$ )

or the control vector group ( $P < 0.05$ ). There is no significant difference between the sham group and the control vector group observed ( $P < 0.05$ , Figures 3 and 4). The results revealed that miR-132/212 cluster inhibits the subcutaneous xenografts of human lung cancer H1299 cells growth via decreasing the expression of Ki67 and the forming of tumor angiogenesis.

### Discussion

Increasing studies elevated that miRNAs play important roles in cancer development, progression, tumor invasion and metastasis [10-13]. miRNAs, including miR-21, miR-221/222, miR-494 and miR-328 are involved in the pathogenesis of non-small cell lung cancer [14, 15]. You *et al.* found that miR-132 was significantly downexpressed in non-small cell lung cancer cells (NSCLC) and in NSCLC clinical specimens [16]. Moreover, miR-132 can inhibit the migration and invasion of NSCLC cancer. Previous reports also found that miR-212 expression is upregulated in lung adenocarcinoma [17]. The overexpression of miR-212 in lung cancer cells promotes cell cycle progression, cell proliferation, migration and invasion [18]. However, the effect of the miR-132/212 cluster on the growth of lung cancer xenografts in nude mice remains unclear. The intensive study of miRNAs in NSCLC may provide new insights for the diagnosis and treatment of lung cancer. Our research established a human lung cancer H1299 cell xenograft model in nude mice and intratumoral injected with miR-132/212 plasmid or control vector plasmid.

## miR-132/212 cluster inhibits lung cancer xenografts proliferation

Tumor growth curve showed that miR132/212 cluster can stop or slow tumor growth compared with the control groups.

To elucidate the mechanism underlying miR-132/212 cluster inhibits tumor growth, we performed immunohistochemistry to detect possible targets for miR-132/212 cluster. Firstly, Ki-67 expression in each group was analyzed and the proliferation index was calculated. We found that the tumor cell proliferation index of the miR-132/212 group was significantly lower than the sham group ( $P < 0.05$ ) or the control vector group ( $P < 0.05$ ), indicating that miR-132/212 cluster significantly inhibited the proliferation of tumor cells. Wu *et al.* found that microRNA-99a, by targeting the fibroblast growth factor receptor-3, inhibited the proliferation, migration and invasion of T24 cells and EJ cells in bladder cancer [19]. miR-132 expression is normally downregulated in ductal carcinoma in situ, whereas miR-132 overexpression can inhibit breast cancer cell line proliferation and colony formation [20]. Zhang *et al.* found that miR-132 overexpression in pancreatic cancer Panc-1 cells inhibited the proliferation of pancreatic cancer cells [21]. However, Park *et al.* found that miR-132/212 cluster can promote the proliferation of pancreatic cancer Panc-1 cells [8], which conflicts with our conclusion. This contradiction effect may be partial due to the differences of genetic background of cell types among the studies.

As we known, P21, which is located in the downstream of P53 gene, is not only related to tumor inhibition but also coordinates the relationships among cell-cycle progression, DNA replication and DNA repair by inhibiting the activity of cyclin-dependent kinase [22], while CyclinD1 promotes the transition from G1 to S phase, accelerates cell-cycle progression and promotes cell proliferation [23]. CyclinD1 overexpression can cause abnormal cell proliferation, leading to tumorigenesis. Immunohistochemistry analysis evaluating the expression levels of P21 and CyclinD1 in tumor tissues from each group showed that P21 was significantly up-expressed in the miR-132/212 group than the control vector group ( $P < 0.05$ ). The expression levels of CyclinD1 in the miR-132/212 group were significantly lower than the control vector group ( $P < 0.05$ ). Previous report found that miR-7 overexpression reduced the expression of CyclinD1 and upregulated the expres-

sion of p21, Caspase-3 and Bax, resulting in proliferation inhibition and advancing apoptosis in colon cancer cells [24]. Overexpression of miR-329 arrests cell-cycle progression from G1 to S phase, inhibits tumor cell proliferation, downregulates CyclinD1 expression, and upregulates P21 expression, and thereby inhibiting tumor cell growth in the LN18 and T98G glioma cell lines [25]. miR-212 inhibits the proliferation of gastric cancer cells by directly inhibiting the expression of retinoblastoma binding protein 2 (RBP2) proteins while upregulating P21 protein expression [26]. miR-132 overexpression in Panc-1 pancreatic cancer cells inhibits CyclinD1 expression [21], which is consistent with our present study.

Numerous researches have focused on the anti-tumor angiogenesis to inhibit tumor growth [27]. Drugs targeting tumor angiogenesis have been applied in clinic [28]. Shi *et al.* found that miR-124 overexpression inhibited glioma xenograft angiogenesis and tumor growth in nude mice [29]. miR-128 overexpression can inhibit the ERK, AKT and P38 signaling pathways as well as tumor angiogenesis and tumor formation by inhibiting the expression of vascular endothelial growth factor (VEGF-C) [30]. In the rat cornea model, miR-132 has a role in promoting angiogenesis [31]. Moreover, miR-132 in several human tumors and in vascular tumors increased Ras activity and stimulated endothelial cell proliferation and angiogenesis by inhibiting the expression of p120 RasGAP [32]. In this study, miR-132/212 cluster inhibited the tumor angiogenesis in human lung H1299 cell xenografts in nude mice. However, the mechanism underlying the miR132/212 cluster inhibits the tumor angiogenesis, either by indirectly inhibiting the expression of tumor angiogenesis factors (TAF) or by directly inhibiting tumor angiogenesis requires further investigation.

Taken together, our results indicated that miR-132/212 cluster inhibits the growth of human lung cancer H1299 cell xenografts in nude mice by up-regulating the expression of P21 and down-regulating the expression of CyclinD1, and thereby inhibiting tumor tissue proliferation and angiogenesis.

### Acknowledgements

This work is Funded by National Natural Science Foundation of China (81402518; 81472920),

Jiangsu Provincial Special Program of Medical Science (BL2012046), Changzhou Social Development Project (CE20125026; CE2013-5050) and Changzhou Scientific Program (ZD-201315; CY20130017).

#### Disclosure of conflict of interest

None.

**Address correspondence to:** Yanzhi Bi, Department of Oncology, Changzhou Tumor Hospital, Soochow University, Changzhou 213001, China; Xifa Zhou, Department of Radiotherapy, Changzhou Tumor Hospital, Soochow University, Changzhou 213001, China. Tel: +86519-86868265; Fax: +86519-8686-8265; E-mail: 623447244@qq.com (YZB); 83559-808@qq.com (XFZ)

#### References

- [1] Lee RC, Feinbaum RL, Ambros V. The C. elegans heterochronic gene lin-4 encodes small RNAs with antisense complementarity to lin-14. *Cell* 1993; 75: 843-854.
- [2] He L, Hannon GJ. MicroRNAs: small RNAs with a big role in gene regulation. *Nat Rev Genet* 2004; 5: 522-531.
- [3] Mendell JT. MicroRNAs: critical regulators of development, cellular physiology and malignancy. *Cell Cycle* 2005; 4: 1179-1184.
- [4] Volinia S, Calin GA, Liu CG, Ambs S, Cimmino A, Petrocca F, Visone R, Iorio M, Roldo C, Ferracin M, Prueitt RL, Yanaihara N, Lanza G, Scarpa A, Vecchione A, Negrini M, Harris CC, Croce CM. A microRNA expression signature of human solid tumors defines cancer gene targets. *Proc Natl Acad Sci U S A* 2006; 103: 2257-2261.
- [5] Tie J, Fan D. Big roles of microRNAs in tumorigenesis and tumor development. *Histol Histopathol* 2011; 26: 1353-1361.
- [6] Ma L, Teruya-Feldstein J, Weinberg RA. Tumour invasion and metastasis initiated by microRNA-10b in breast cancer. *Nature* 2007; 449: 682-688.
- [7] Jin W, Reddy MA, Chen Z, Putta S, Lanting L, Kato M, Park JT, Chandra M, Wang C, Tangirala RK, Natarajan R. Small RNA sequencing reveals microRNAs that modulate angiotensin II effects in vascular smooth muscle cells. *J Biol Chem* 2012; 287: 15672-15683.
- [8] Park JK, Henry JC, Jiang J, Esau C, Gusev Y, Lerner MR, Postier RG, Brackett DJ, Schmittgen TD. miR-132 and miR-212 are increased in pancreatic cancer and target the retinoblastoma tumor suppressor. *Biochem Biophys Res Commun* 2011; 406: 518-523.
- [9] Luo J, Zhou X, Ge X, Liu P, Cao J, Lu X, Ling Y, Zhang S. Upregulation of Ying Yang 1 (YY1) suppresses esophageal squamous cell carcinoma development through heme oxygenase-1. *Cancer Sci* 2013; 104: 1544-1551.
- [10] Wang QY, Tang J, Zhou CX, Zhao Q. [The down-regulation of miR-129 in breast cancer and its effect on breast cancer migration and motility]. *Sheng Li Xue Bao* 2012; 64: 403-411.
- [11] Suzuki H, Tokino T, Shinomura Y, Imai K, Toyota M. DNA methylation and cancer pathways in gastrointestinal tumors. *Pharmacogenomics* 2008; 9: 1917-1928.
- [12] Wang J, Gu Z, Ni P, Qiao Y, Chen C, Liu X, Lin J, Chen N, Fan Q. NF-kappaB P50/P65 heterodimer mediates differential regulation of CD-166/ALCAM expression via interaction with microRNA-9 after serum deprivation, providing evidence for a novel negative auto-regulatory loop. *Nucleic Acids Res* 2011; 39: 6440-6455.
- [13] Wang J, Sen S. MicroRNA functional network in pancreatic cancer: from biology to biomarkers of disease. *J Biosci* 2011; 36: 481-491.
- [14] Qi J, Mu D. MicroRNAs and lung cancers: from pathogenesis to clinical implications. *Front Med* 2012; 6: 134-155.
- [15] Zhang JG, Wang JJ, Zhao F, Liu Q, Jiang K, Yang GH. MicroRNA-21 (miR-21) represses tumor suppressor PTEN and promotes growth and invasion in non-small cell lung cancer (NSCLC). *Clin Chim Acta* 2010; 411: 846-852.
- [16] You J, Li Y, Fang N, Liu B, Zu L, Chang R, Li X, Zhou Q. MiR-132 suppresses the migration and invasion of lung cancer cells via targeting the EMT regulator ZEB2. *PLoS One* 2014; 9: e91827.
- [17] Rabinowits G, Gercel-Taylor C, Day JM, Taylor DD, Kloecker GH. Exosomal microRNA: a diagnostic marker for lung cancer. *Clin Lung Cancer* 2009; 10: 42-46.
- [18] Li Y, Zhang D, Chen C, Ruan Z, Huang Y. MicroRNA-212 displays tumor-promoting properties in non-small cell lung cancer cells and targets the hedgehog pathway receptor PTCH1. *Mol Biol Cell* 2012; 23: 1423-1434.
- [19] Wu D, Zhou Y, Pan H, Zhou J, Fan Y, Qu P. microRNA-99a inhibiting cell proliferation, migration and invasion by targeting fibroblast growth factor receptor 3 in bladder cancer. *Oncol Lett* 2014; 7: 1219-1224.
- [20] Li S, Meng H, Zhou F, Zhai L, Zhang L, Gu F, Fan Y, Lang R, Fu L, Gu L, Qi L. MicroRNA-132 is frequently down-regulated in ductal carcinoma in situ (DCIS) of breast and acts as a tumor suppressor by inhibiting cell proliferation. *Pathol Res Pract* 2013; 209: 179-183.
- [21] Zhang S, Hao J, Xie F, Hu X, Liu C, Tong J, Zhou J, Wu J, Shao C. Downregulation of miR-132 by promoter methylation contributes to pancreatic cancer development. *Carcinogenesis* 2011; 32: 1183-1189.

## miR-132/212 cluster inhibits lung cancer xenografts proliferation

- [22] Kim J, Bae S, An S, Park JK, Kim EM, Hwang SG, Kim WJ, Um HD. Cooperative actions of p21WAF1 and p53 induce Slug protein degradation and suppress cell invasion. *EMBO Rep* 2014; 15: 1062-8.
- [23] Lee JY, Lee NK. Up-regulation of cyclinD1 and Bcl2A1 by insulin is involved in osteoclast proliferation. *Life Sci* 2014; 114: 57-61.
- [24] Xu K, Chen Z, Qin C, Song X. miR-7 inhibits colorectal cancer cell proliferation and induces apoptosis by targeting XRCC2. *Onco Targets Ther* 2014; 7: 325-332.
- [25] Xiao B, Tan L, He B, Liu Z, Xu R. MiRNA-329 targeting E2F1 inhibits cell proliferation in glioma cells. *J Transl Med* 2013; 11: 172.
- [26] Jiping Z, Ming F, Lixiang W, Xiuming L, Yuqun S, Han Y, Zhifang L, Yundong S, Shili L, Chunyan C, Jihui J. MicroRNA-212 inhibits proliferation of gastric cancer by directly repressing retinoblastoma binding protein 2. *J Cell Biochem* 2013; 114: 2666-2672.
- [27] Ghavamipour F, Shirin Shahangian S, Sajedi RH, Shahriar Arab S, Mansouri K, Aghamaali MR. Development of highly potent anti-angiogenic VEGF heterodimer by directed blocking of its VEGFR-2 binding site. *FEBS J* 2014; 281: 4479-94.
- [28] Ameratunga M, Pavlakis N, GebSKI V, Broad A, Khasraw M. Epidermal growth factor receptor-tyrosine kinase inhibitors in advanced squamous cell carcinoma of the lung: A meta-analysis. *Asia Pac J Clin Oncol* 2014; 10: 273-278.
- [29] Shi Z, Chen Q, Li C, Wang L, Qian X, Jiang C, Liu X, Wang X, Li H, Kang C, Jiang T, Liu LZ, You Y, Liu N, Jiang BH. MiR-124 governs glioma growth and angiogenesis and enhances chemosensitivity by targeting R-Ras and N-Ras. *Neuro Oncol* 2014; 16: 1341-53.
- [30] Hu J, Cheng Y, Li Y, Jin Z, Pan Y, Liu G, Fu S, Zhang Y, Feng K, Feng Y. microRNA-128 plays a critical role in human non-small cell lung cancer tumorigenesis, angiogenesis and lymphangiogenesis by directly targeting vascular endothelial growth factor-C. *Eur J Cancer* 2014; 50: 2336-2350.
- [31] Mulik S, Xu J, Reddy PB, Rajasagi NK, Gimenez F, Sharma S, Lu PY, Rouse BT. Role of miR-132 in angiogenesis after ocular infection with herpes simplex virus. *Am J Pathol* 2012; 181: 525-534.
- [32] Anand S, Majeti BK, Acevedo LM, Murphy EA, Mukthavaram R, Scheppke L, Huang M, Shields DJ, Lindquist JN, Lapinski PE, King PD, Weis SM, Cheresch DA. MicroRNA-132-mediated loss of p120RasGAP activates the endothelium to facilitate pathological angiogenesis. *Nat Med* 2010; 16: 909-914.